

Sting Effects on Transonic Delta Wing Experiments

L.A.Schiavetta

University of Glasgow, Glasgow, UK,

O.J.Boelens

National Aerospace Laboratory, NLR, Amsterdam, The Netherlands

W.Fritz

EADS Military Air Systems, Munich, Germany

R.M.Cummings

United States Air Force Academy, Colorado Springs, CO, USA,

It has been observed that delta wings placed in a transonic freestream can experience a sudden movement of the vortex breakdown location as the angle of incidence is increased. The current paper uses CFD to explain this behaviour in detail. The study shows that a shock-vortex interaction is responsible, with the shock arising from the presence of a sting in the supersonic flow over the wing. The balance of the vortex strength and axial flow, and the shock strength, is examined to provide an explanation of the sensitivity of the breakdown location. Limited experimental data is available to supplement the CFD results in certain key respects, and the ideal synergy between CFD and experiments for this problem is considered.

I. Introduction

The occurrence of shocks on delta wings introduces complex shock/vortex interactions, particularly at moderate to high angles of incidence. These interactions can make a significant difference to the vortex breakdown behaviour. For subsonic flows the motion of the location of onset of breakdown towards the apex is relatively gradual with increasing incidence.¹ The strengthening of the shock which stands off the sting as the incidence is increased can lead to a shock/vortex interaction triggering breakdown. The location of breakdown can shift upstream by as much as 30% of the chord in a single 1° incidence interval^{2,3} due to this interaction.

From the study of the interaction between longitudinal vortices and normal shocks in supersonic flow⁴ it has been found that it is possible for a vortex to pass through a normal shock without being weakened sufficiently to cause breakdown. However, the flow over slender delta wings is more complex as the shock does not appear to be normal to the freestream in the vortex core region.⁵ Therefore, further investigation is needed to consider the behaviour and onset of vortex breakdown, particularly with respect to shock/vortex interactions.

To consider this behaviour, the flow over a sharp leading edged, slender delta wing was considered under subsonic and transonic conditions. This investigation was undertaken as part of the 2nd International Vortex Flow Experiment (VFE-2), a facet of the NATO RTO AVT-113 Task Group, which was set up to consider the flow behaviour both experimentally and computationally over a specified 65° delta wing geometry. The work of the VFE-2 continues on from the first International Vortex Flow Experiment (VFE-1)⁶ carried out in the late eighties, which was used to validate the inviscid CFD codes of the time. Much progress has been made in both experimental and computational aerodynamics, particularly in turbulence models since the conclusion of the VFE-1. Therefore, it was proposed by Hummel and Redecker⁷ that a second experiment should be undertaken to provide a new, comprehensive database of results for various test conditions and flow behaviours,

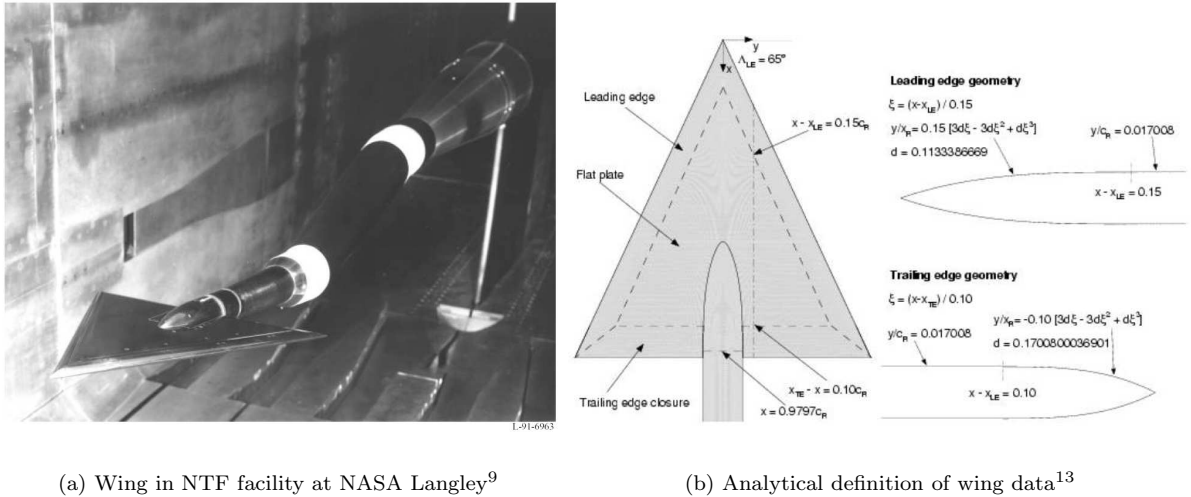
Report Documentation Page				Form Approved OMB No. 0704-0188	
Public reporting burden for the collection of information is estimated to average 1 hour per response, including the time for reviewing instructions, searching existing data sources, gathering and maintaining the data needed, and completing and reviewing the collection of information. Send comments regarding this burden estimate or any other aspect of this collection of information, including suggestions for reducing this burden, to Washington Headquarters Services, Directorate for Information Operations and Reports, 1215 Jefferson Davis Highway, Suite 1204, Arlington VA 22202-4302. Respondents should be aware that notwithstanding any other provision of law, no person shall be subject to a penalty for failing to comply with a collection of information if it does not display a currently valid OMB control number.					
1. REPORT DATE JUN 2007		2. REPORT TYPE N/A		3. DATES COVERED -	
4. TITLE AND SUBTITLE Sting Effects on Transonic Delta Wing Experiments				5a. CONTRACT NUMBER	
				5b. GRANT NUMBER	
				5c. PROGRAM ELEMENT NUMBER	
6. AUTHOR(S)				5d. PROJECT NUMBER	
				5e. TASK NUMBER	
				5f. WORK UNIT NUMBER	
7. PERFORMING ORGANIZATION NAME(S) AND ADDRESS(ES) United States Air Force Academy, Colorado Springs, CO, USA				8. PERFORMING ORGANIZATION REPORT NUMBER	
9. SPONSORING/MONITORING AGENCY NAME(S) AND ADDRESS(ES)				10. SPONSOR/MONITOR'S ACRONYM(S)	
				11. SPONSOR/MONITOR'S REPORT NUMBER(S)	
12. DISTRIBUTION/AVAILABILITY STATEMENT Approved for public release, distribution unlimited					
13. SUPPLEMENTARY NOTES Third International Symposium on Integrating CFD and Experiments in Aerodynamics, June 2007, The original document contains color images.					
14. ABSTRACT					
15. SUBJECT TERMS					
16. SECURITY CLASSIFICATION OF:			17. LIMITATION OF ABSTRACT UU	18. NUMBER OF PAGES 17	19a. NAME OF RESPONSIBLE PERSON
a. REPORT unclassified	b. ABSTRACT unclassified	c. THIS PAGE unclassified			

to further the understanding of vortical flows. The test conditions considered under the VFE-2 framework include both subsonic and transonic Mach numbers for low, medium and high angles of incidence at a range of Reynolds numbers.⁸

The measured transonic data showed a sudden jump of the breakdown location towards the wing apex when a critical angle of incidence was reached. The current study uses CFD to investigate this effect towards an explanation of the detailed factors contributing to this behaviour. The paper continues with a description of the test case and observed experimental behaviour. A summary of a wide ranging CFD study is then presented. Finally, the combined results are considered to produce an assessment of the mechanisms driving the flow behaviour.

II. Experiments

The geometry used for the VFE-2 was originally tested in experiments carried out by Chu and Luckring⁹⁻¹² in the National Transonic Facility (NTF) at NASA Langley. These experiments considered a 65° delta wing with four leading edge profiles (one sharp and three rounded with small, medium and large radii) for a wide range of conditions both subsonic and transonic and for both test and flight Reynolds numbers. This data has been compiled into a comprehensive experimental database and forms the basis for the investigations of the VFE-2. The geometry is analytically defined for all leading edge profiles. Both the medium radius and sharp leading edge profiles are considered within VFE-2, however, for this investigation, only the sharp leading edge profile is considered. Figure 1 shows the wing situated in the NTF wind tunnel and a brief overview of the analytical dimensions of the wing.



(a) Wing in NTF facility at NASA Langley⁹

(b) Analytical definition of wing data¹³

Figure 1. VFE-2 65° delta wing geometry used in investigation

The location of vortex breakdown for a freestream Mach number of 0.85 with incidence measured in the NTF⁹ and DLR¹⁴ experiments is plotted in Figure 2. The CFD data also plotted in this figure is discussed later in this paper. For the experimental data, the exact location of vortex breakdown is not known, however from the surface pressure coefficient distributions the approximate locations could be determined. The behaviour of vortex breakdown is clear, with a sudden movement of the breakdown location towards the apex when a critical angle is reached. It is however difficult to see why this happens from the measured data available. In particular, at least a larger density of pressure measurements is needed. In fact it is seen from the CFD study that flowfield data is also needed to reveal details of the state of the vortex.

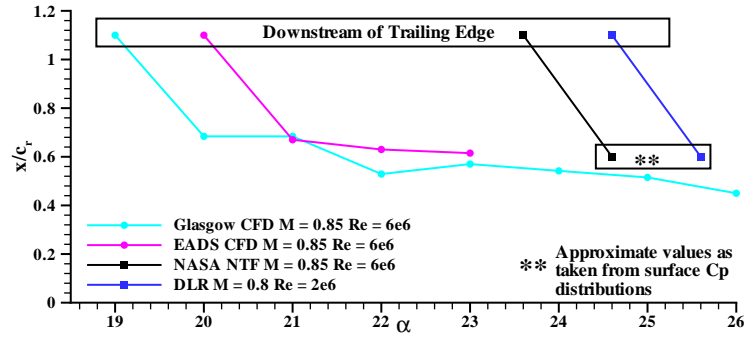


Figure 2. Vortex breakdown location for both computational and experimental results

III. CFD Study

A CFD study was undertaken using several codes, grids and modelling options. The purpose of this study was to see if the behaviour observed in the measurements (i.e. the sudden jump in breakdown towards the apex) could be predicted, and if so with what sensitivity to the details of the simulation. Detailed descriptions of the flow solvers, computational set-up and grids used in the structured grid comparisons can be found in Ref.¹⁵ and are summarised in Table 1.

<i>Institution</i>	<i>Topology</i>	<i>Size</i> $\times 10^6$	<i>No. of Grid Points on Wing</i>			<i>Turbulence Model</i>
			<i>Spanwise</i>	<i>Streamwise</i>	<i>Normal</i>	
EADS ¹⁶	C-O	~ 10.6	129	257	129	Wilcox k- ω and Reynolds Stress Model
NLR ^{17,18}	C-O	~ 4	192	112	96	TNT k- ω with P_ω Enhancer
Glasgow ¹⁹	H-H with O-grid	~ 7	170 (117)	228 (171)	81 (49)	Wilcox k- ω with P_ω Enhancer and NLEVM

Table 1. Summary of grids and turbulence models used for VFE-2 structured grid comparisons. Coarse grid dimensions are given in parentheses for the Glasgow code.

The effect of time accuracy is considered by comparing the steady solutions to those of the USAFA²⁰ using the Spalart-Allmaras DES turbulence treatment on a unstructured grid. The grid used had approximately 7.89×10^6 cells and an average first wall spacing of $y^+ = 0.68$, created specifically for a Reynolds number of 6×10^6 . It was refined within the vortex core region to improve the grid for the application of DES. A non-dimensional time step of $\Delta\tau \approx 0.0047$ was used and the calculation was allowed to run for approximately 20600 time steps. For the comparisons, both instantaneous and time averaged (mean) solutions were necessary and thus, a time averaged file was created over a total of 4000 time steps.

A. Subsonic Results

First, a case at a freestream Mach number of 0.4 was computed. This case has no shock waves present. Two angles of incidence were calculated (at 18.5 degrees where no breakdown is present over the wing and at 23 degrees where it is) and compared with the NTF measurements. Sample results are shown in figure 3 which compares the predictions of the Glasgow, NLR and EADS simulations, with excellent agreement between all predictions and the measurements. This is typical of the expected performance of CFD codes for the prediction of pressures on a sharp edged delta wing in subsonic flow, even if breakdown is present.

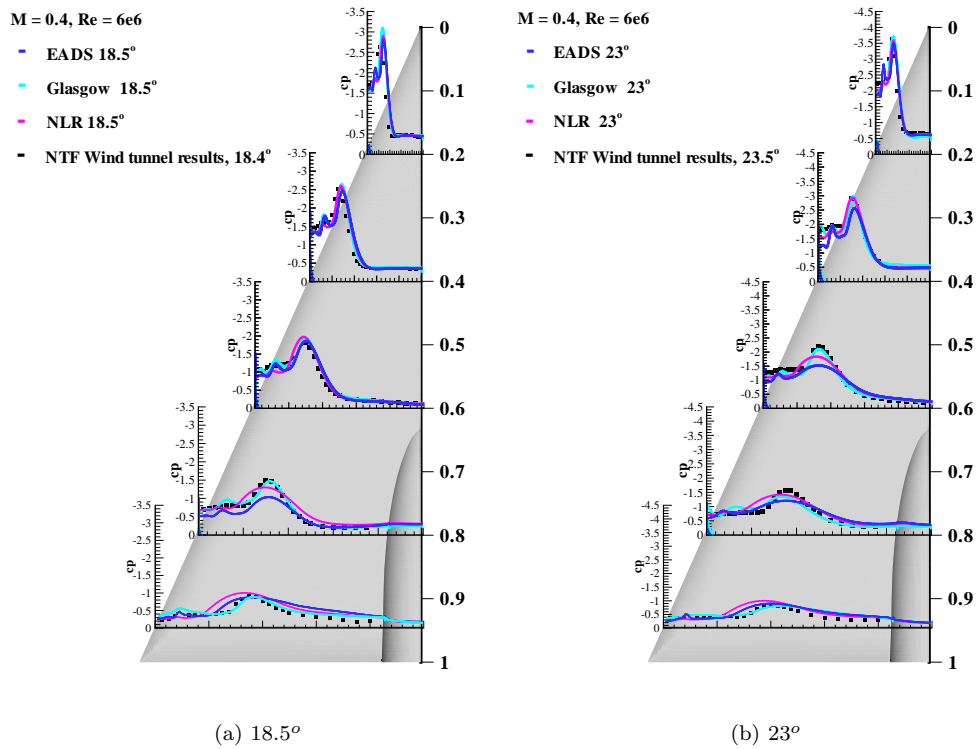


Figure 3. Comparison of computational results and experimental data, $M = 0.4$ and $Re = 6 \times 10^6$

B. Transonic Results

Next, cases with a freestream Mach number of 0.85 were considered. Here there are shock waves present. The same angles of incidence were computed, with 18 degrees again giving no breakdown over the wing and 23 degrees resulting in breakdown. The comparisons are shown in figure 4. The case before breakdown shows similar levels of agreement with the measurements. However, the case after breakdown shows significant discrepancies arising from the premature prediction of vortex breakdown. In fact the sudden movement of breakdown is predicted about 3 degrees earlier for the CFD when compared with the measurements.

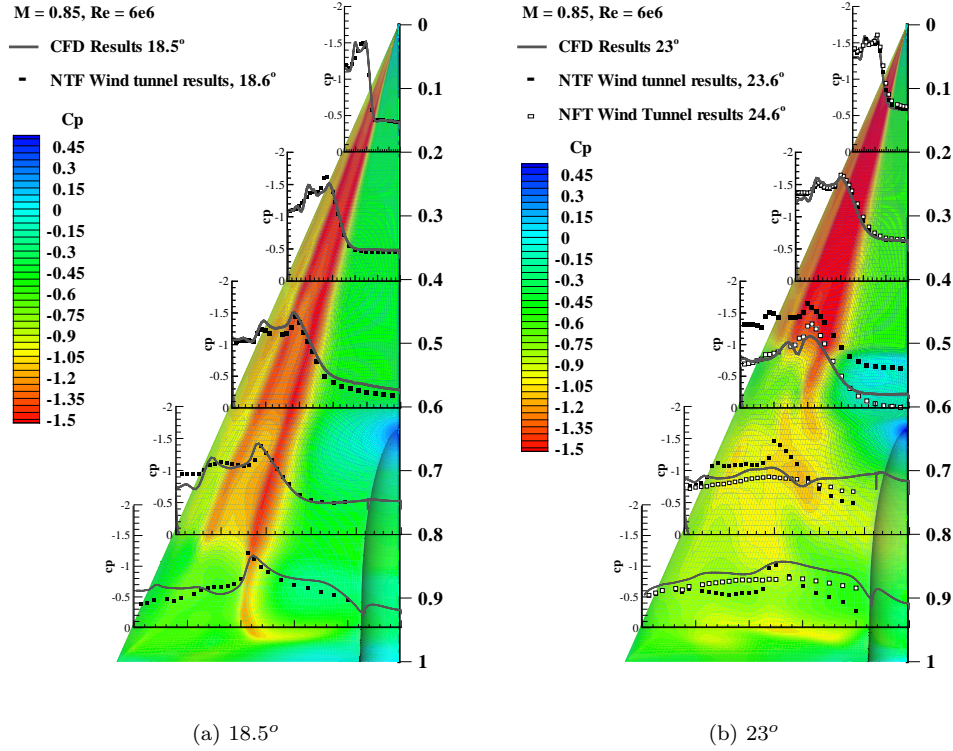


Figure 4. Comparison of computational results and experimental data, $M = 0.85$ and $Re = 6 \times 10^6$

C. Location of Shock Waves

Normal and crossflow shocks were found to occur in this flow. The main focus here is on the normal shocks, which can be identified by plotting the pressure coefficient along the symmetry plane as shown in Figure 5 for both angles of incidence. For the 18.5° case, it is clear that two normal shocks occur at the symmetry plane. The first occurs upstream of the sting tip at approximately $x/c_r = 0.6$, which is most likely to be caused by the sting geometry. Further downstream at approximately $x/c_r = 0.85$ a second shock is found. This second shock is likely to correspond to the rear/terminating shock as described in the literature^{2, 5, 21} for similar conditions. A third compression region is also found close to the trailing edge, and a third shock is found from the surface pressure contours at this location outboard of the symmetry plane on the wing surface. A shock occurring at this location is likely to be caused by the high curvature of the wing geometry and the necessity of the flow to return to freestream conditions at the trailing edge.

As the incidence is increased and vortex breakdown occurs on the wing, the behaviour at the symmetry plane, again, shows the shock at the sting tip at approximately $x/c_r = 0.6$.

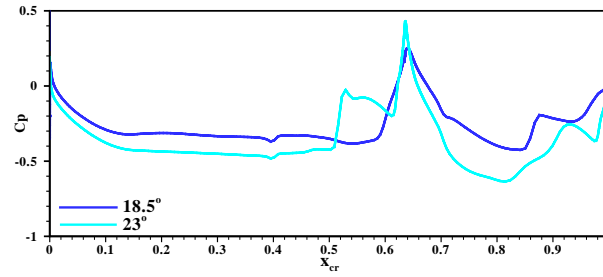


Figure 5. Pressure coefficient distribution from Glasgow code at the symmetry plane on the wing for both angles of incidence

However, another shock is also found in the flow slightly upstream of this location at about $x/c_r = 0.52$. Downstream of the sting tip, it is evident that the rear/terminating shock described for the $\alpha = 18.5^\circ$ case is no longer present. From the behaviour described in the investigations of Elsenaar and Hoeijmakers² under similar conditions, it is possible that the new shock upstream of the sting tip is the rear/terminating shock having undergone an upstream shift with the increase of incidence. As before, it is found that three normal shocks occur at the symmetry plane and close to the trailing edge, as also found in the experiments, a second normal shock is observed.

Considering the three-dimensional behaviour of the normal shocks, it is found that the shock occurring upstream of the sting tip curves downstream and intersects the rolled up shear layer of the vortex as shown in Figure 6 and highlighted by the dashed lines. This is also in agreement with the observations of Donohoe and Bannink.⁵ Also highlighted are the locations of the other normal shocks described above. The rear/terminating shock in the 18.5° solution is found to be normal to the freestream and wing surface and does not appear to curve downstream outboard of the symmetry plane. This lack of curvature may be due to the influence of the sting, as previous investigations have considered a flat wing without sting support.⁵

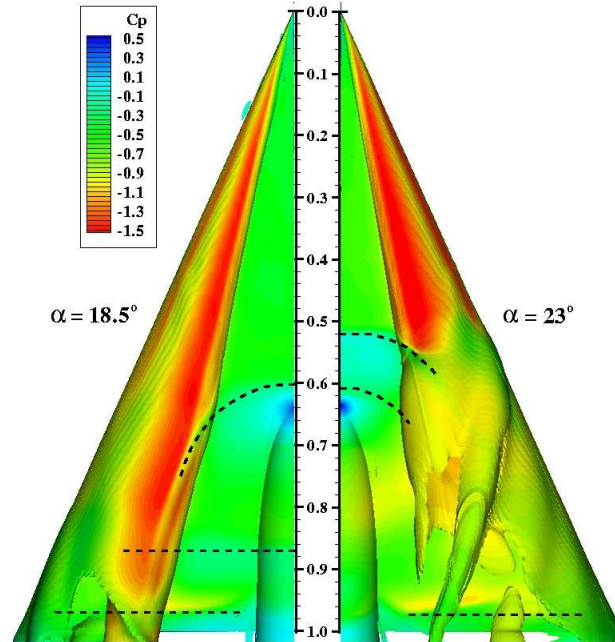


Figure 6. Isosurface of x vorticity coloured by pressure coefficient showing primary vortex shear layer and normal shock shape for both angles of incidence (from the Glasgow code)

D. Sensitivity Study

A sensitivity study was carried out to assess the CFD predictions of the sudden motion of the breakdown location. A large number of calculations are only summarised here. The conclusion in all cases is that the sudden motion of the breakdown location was present no matter what the details of the calculation used, and that the critical angle is predicted to be lower in the computations than in the measurements.

1. Effect of Grid Refinement

The effect of grid refinement was considered for both pre- and post-breakdown flow for the transonic conditions using the Glasgow results. Comparisons of the surface pressure coefficient distributions for both angles of incidence with the relevant experimental data are shown in Figure 7. There are some differences in detail between the two solutions.

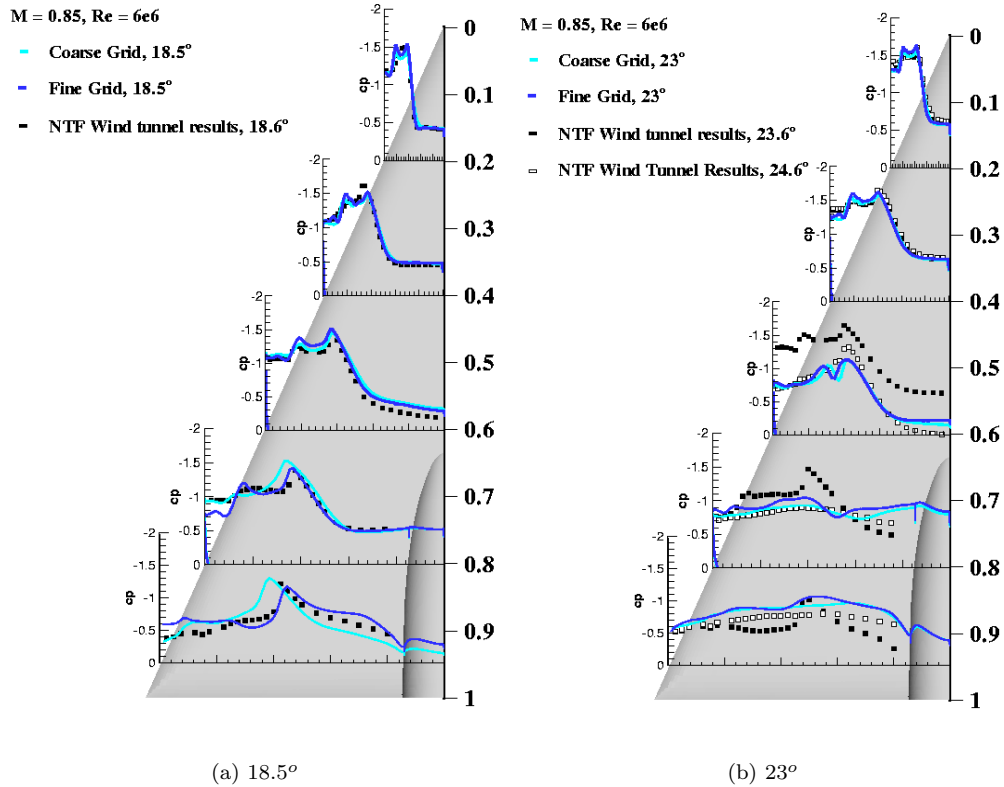


Figure 7. Comparison between the H-H grids for transonic conditions at $\alpha = 18.5^\circ$ and 23° from the Glasgow code.

However, the behaviour and location of vortex breakdown are not greatly affected by the grid refinement carried out. It is also the case that the critical angle for vortex breakdown onset is independent of the grid refinement used, with vortex breakdown predicted to occur at lower angles of incidence on both grids.

2. Effect of Turbulence Model

The effect of the turbulence model on the flow behaviour was considered by comparing results calculated using the $k-\omega$ with P_ω Enhancer model and the Non-Linear Eddy Viscosity model in the Glasgow code, and the standard Wilcox $k-\omega$ and a Reynolds Stress model (RSM) by EADS. The surface pressure coefficients are shown in figure 8. Each model predicts breakdown to occur on the wing at an incidence which is lower than that witnessed in the experiment. Some differences in the breakdown location are present due

to the different vortex strengths predicted. However, the behaviour of a rapid motion forward of the breakdown location is the same in each case.

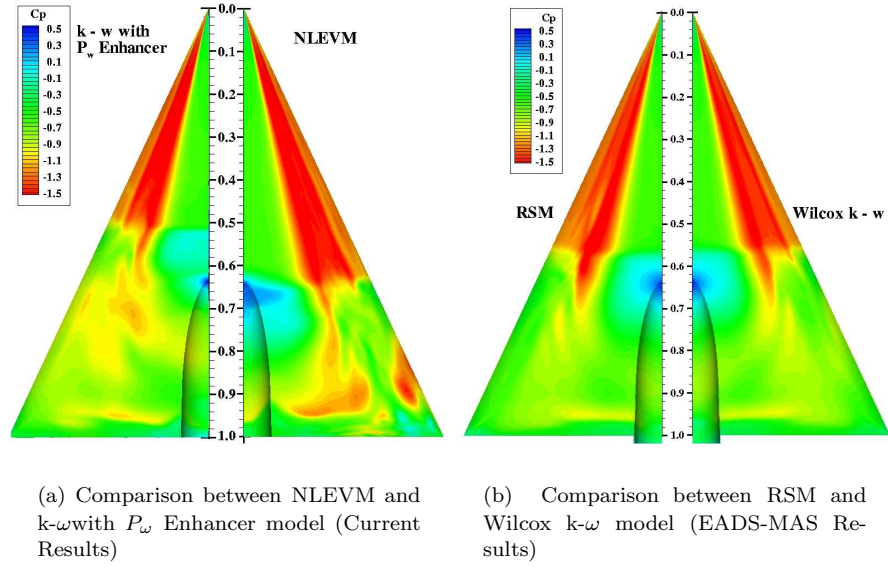


Figure 8. Contours of surface pressure coefficient showing effect of turbulence model on flow solution with comparison to experiment for $\alpha = 23^\circ$, $M = 0.85$ and $Re = 6 \times 10^6$

3. Comparison of Structured Grid Results

Comparison of the structured solutions obtained at Glasgow, NLR and EADS was made. The locations of the normal shocks in the flow solutions, and the vortex breakdown locations, are slightly different for each solution, as shown in figure 9. These are likely due to the slightly different turbulence treatments and grids. However, the motion of the breakdown location is very similar in each case.

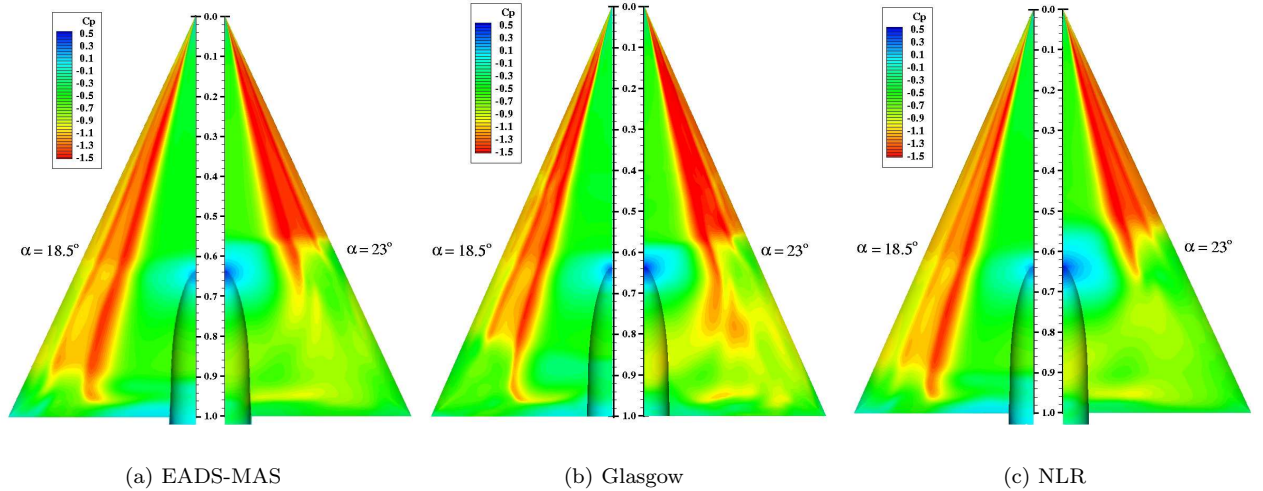


Figure 9. Surface pressure coefficient contours for all codes, $M = 0.85$, $Re = 6 \times 10^6$

A comparison between the solutions for the Glasgow and NLR CFD solvers on a common grid was also performed. The turbulence models used by these two institutions are

similar, with the difference mainly in the specification of the turbulence model diffusion coefficients.²² The solutions obtained were very similar.

4. Influence of Time Accuracy

Figure 10 shows the comparison of surface pressure coefficient distributions for the time averaged USAFA solutions and the steady state Glasgow solution. Again, there are some differences in breakdown location and the shock strength. However, again the behaviour of the breakdown location motion is very similar in both cases.

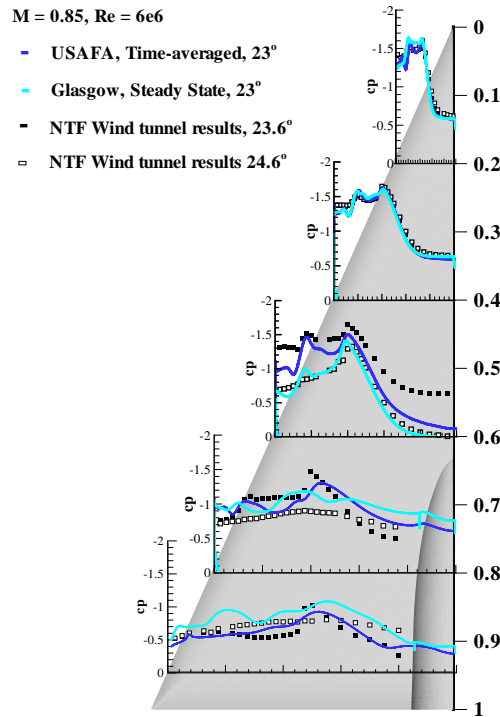


Figure 10. Comparisons between computational results and experiment for current results and USAFA time accurate solutions for $\alpha = 23^\circ$, $M = 0.85$, $Re = 6 \times 10^6$

IV. Evaluation

From the CFD results presented the sting tip shock intersects the vortex system. It therefore seems possible that a shock/vortex interaction takes place, particularly for higher angles of incidence. To consider this, the pressure in the freestream direction through the vortex cores for both angles of incidence were analysed. This is shown in Figure 11, with the calculated pressure ratios for each shock/vortex interaction location marked. For $\alpha = 18.5^\circ$, the interactions occur without vortex breakdown. It has been previously suggested that this is due to the shock sitting above the vortex core.⁵ However, from consideration of the vortex core properties it is found that there are three regions of adverse pressure gradient which may suggest direct interactions. These coincide with the two normal shocks at the symmetry plane and the trailing edge shock, detailed previously, and are clear from the three dimensional view in Figure 6. The pressure ratios for all three are less than 1.5 and, as shown, the primary vortex recovers after passing through each. Therefore, it may be suggested that these are weak interactions.

At $\alpha = 23^\circ$, where breakdown occurs on the wing, it is clear that there are two regions of high adverse pressure gradient at the vortex core. The first coincides with the location of the normal shock upstream of the sting tip as shown at the symmetry plane in Figure 5 and also with the onset of vortex breakdown. Very close to this, the second, higher pressure

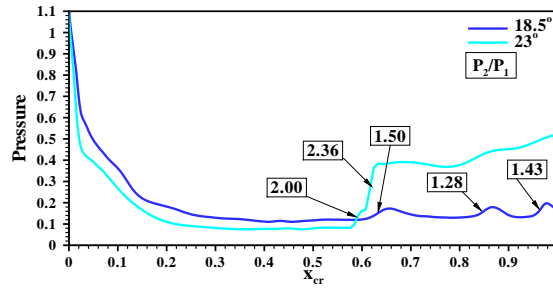


Figure 11. Pressure distribution (from the Glasgow code) through vortex cores for both angles of incidence; The numbers on the plot signify the magnitudes of the pressure ratios through the intersecting shocks

gradient coincides with the occurrence of complete vortex breakdown. These pressure gradients have ratios of 2.00 and 2.36 respectively. It is likely that the first pressure increase is due to the effect of the normal shock at the symmetry plane on the vortex core, in a similar manner to the interaction at the lower incidence.

From these results, it is evident that there are interactions between the shocks and vortex core for both angles of incidence, with a weaker interaction occurring for the lower incidence. Thus, it may be suggested that there is a limiting behaviour below which the vortex can retard the effects of the shock and remain coherent. Above this limit, the interaction causes a considerable weakening of the vortex core, which results in vortex breakdown. In his comprehensive review, Deléry²³ demonstrated the importance of a number of parameters for vortex breakdown caused by shock/vortex interaction. These include the tangential or swirl velocity, U_θ , and the axial velocity of the vortex core, U_{axial} . He also proposed that the swirl ratio or the Rossby number may be used as a measure of the vortex intensity and, thus, the susceptibility of the vortex to shock induced breakdown. The Rossby number is a non-dimensional parameter, defined as the ratio of the axial and circumferential momentum in a vortex as defined by Equation 1. In this investigation, the maximum axial velocity at the vortex core and the maximum swirl velocity of the vortex are used. This relationship is the inverse of the axial swirl parameter,²³ which is used as a breakdown criterion for a free-vortex.

$$Ro = \frac{U_{axial}}{r_c \Omega} = \frac{U_{axial}}{U_\theta} \quad (1)$$

As a vortex passes through a normal shock, the tangential velocity is found to stay relatively constant while the axial velocity decreases, therefore reducing the Rossby number.²⁴ With the reduction in the Rossby number comes an increase in vortex intensity and, as a result, the susceptibility of the vortex to breakdown increases. A criterion for breakdown using the Rossby number has also been investigated by Spall *et al.*²⁵ and by Robinson *et al.*,²⁶ who applied it to computational results on slender delta wings and determined that the limiting Rossby number occurs between 0.9 and 1.4 for most cases, with a stable vortex core occurring for values above 1.4. To consider this criterion, the Rossby number was calculated for both pre- and post-breakdown angles of incidence and the resulting graph is shown in Figure 12 with respect to streamwise location on the wing. Also noted on the plot are the critical Rossby numbers for vortex breakdown.

These results also show the influence of the shocks on the vortex behaviour. At $\alpha = 18.5^\circ$, it is clear that weak interactions occur as the Rossby number decreases. However, this reduction is not significant which shows that the vortex is not sufficiently weakened by the shock. A recovery is witnessed downstream. At $\alpha = 23^\circ$, a similar behaviour is noted where at $x/c_r = 0.58$ the vortex is affected by the normal shock. However, the reduction in Rossby number is greater than for $\alpha = 18.5^\circ$ and the vortex becomes unstable. Vortex breakdown is then caused by a second shock at approximately $x/c_r = 0.62$ which has a greater effect on the already weakened vortex flow, and breakdown is almost immediate.

To investigate a limit for transonic delta wing vortices, the strength of the impinging shocks should be considered, pre- and post-breakdown. Unfortunately, little experimental data exists to allow the shock strength to be measured through the vortex core. However, the strength of the shocks incident on the surface of the wing may be considered to improve confidence in the computational solutions. For the NASA NTF experimental results, the

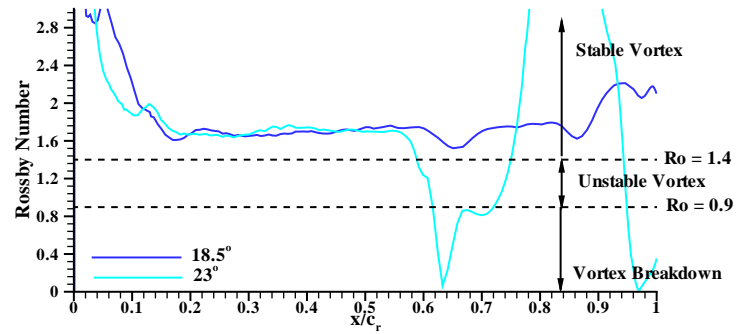


Figure 12. Rossby number distribution from the Glasgow code against root chord location for pre- and post-breakdown cases

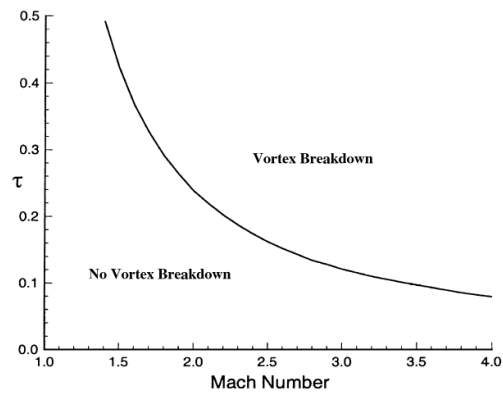


Figure 13. Theoretical limit curve for normal shock vortex interactions, where τ is the swirl ratio $= 1/Ro$ (adapted from Ref [24])

pressure distributions on the surface of the wing at a constant spanwise location of $y/s = 0.3$ were considered for the 23.6° and 24.6° angles of incidence and are shown in Figure 14. Unfortunately, there are only five data points, however, the presence of an increase in pressure between $x/c_r = 0.6$ and 0.8 for the 23.6° incidence and $x/c_r = 0.4$ and 0.6 for the 24.6° incidence is still clear. As the sting tip is located at approximately $x/c_r = 0.64$, these pressure jumps are most likely to be located close to the $x/c_r = 0.6$ streamwise location. Using this as a guide, an approximation to the shock strength at this location can be determined. The approximate values calculated are given in Table 2.

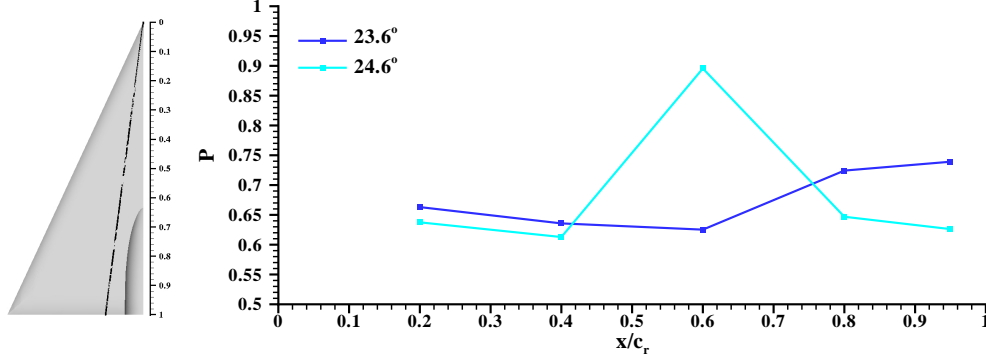


Figure 14. Experimental surface pressure data on conical ray at constant $y/s = 0.3$ to show experimental shock strength for $\alpha = 23.6^\circ$ and 24.6° , $M = 0.85$, $Re = 6 \times 10^6$ from NASA NTF data

	$\frac{P_2}{P_1}$
NASA NTF Experiment - 23.6°	1.16
NASA NTF Experiment - 24.6°	1.4673
CFD - 18.5°	1.2314
CFD - 23°	1.4695

Table 2. Summary of shock strength from the Glasgow code on surface conical ray at constant $y/s = 0.3$ for all solutions at $M = 0.85$, $Re = 6 \times 10^6$ and $\alpha = 23^\circ$ compared to NASA NTF data.

Using the values in Table 2 as a guide, it is evident that there is a considerable difference in the calculated pressure changes at the sting tip location for the pre- and post-breakdown experimental results. The calculated pressure ratio for the post-breakdown case is roughly 25% larger than for the pre-breakdown case. Similar distributions were also obtained from the computational solutions for the pre- and post-breakdown cases and the shock strengths calculated are also stated in Table 2. From a comparison with the experimental data it is clear that the magnitude of the post-breakdown pressure ratio is very similar, however, the pre-breakdown ratio is larger. This means that overall the increase between the pre- and post-breakdown cases for the computational results is less. The larger pressure ratio of the computational results for the pre-breakdown case may have implications for the onset of breakdown. If the shock strength is over-predicted in the computational results, it is likely that breakdown would occur earlier on the wing compared to the experimental results for a given vortex strength.

To consider the incidence at which vortex breakdown first occurs on the wing and relative strength of the shocks in the flow, additional calculations were performed for intermediate angles of incidence between 18.5° and 26° for the same flow conditions as before ($M = 0.85$ and $Re = 6 \times 10^6$). A summary of the important flow details are shown in Table 3. These details include whether vortex breakdown occurred, the maximum vortex core axial velocity, Mach number and the strengths and locations of the first impinging shock at each incidence. The location of the shocks can be taken as analogous to the vortex breakdown location, where appropriate. From the analysis, it was found that the 23° case was the only incidence to exhibit the double shock at vortex breakdown and so

the combined shock strength is instead shown for comparison with the other results.

α	VBD?	Max. U_{axial}	Max. M_{axial}	$\frac{P_2}{P_1}$	Shock x/c_r
18.5°	×	1.74	1.76	1.5	0.62
19°	×	1.76	1.80	1.67	0.64
20°	✓	1.74	1.83	3.73	0.64
21°	✓	1.74	1.86	4.87	0.64
22°	✓	1.79	1.88	4.67	0.51
23°	✓	1.80	1.92	5.25	0.55
24°	✓	1.84	2.05	5.93	0.49
25°	✓	1.84	2.10	5.64	0.47
26°	✓	1.84	2.20	5.48	0.40

Table 3. Summary of shock and vortex core data for all steady state calculations using the Glasgow code at $\alpha = 18.5^\circ - 26^\circ$, $M = 0.85$ and $Re = 6 \times 10^6$ † indicates further converged solution results.

Before considering the onset of breakdown, it is important to note the behaviour of the flow variables with increasing incidence. It is clear from Table 3, that the predicted shock strength increases with incidence, which is in agreement with the experimental data in Table 2. The axial velocity and Mach number are also found to increase, however, the Rossby number was found to be consistent at ≈ 1.7 for each incidence as described before. From the theory of supersonic flows, it is known that the strength of a shock is dependent on the upstream Mach number, thus for a higher axial flow, a stronger shock will occur. However, in this case the relationship does not appear to be linear. This is most likely to be due to changes in the shape of the shock in response to changes in the flow behaviour and the equilibrium conditions as the incidence is increased. This may also suggest that the behaviour of the vortex breakdown is also non-linear in nature.

Vortex breakdown first appears on the wing at $\alpha = 20^\circ$, which coincides with a significant increase in shock strength. At this point it may be assumed that the strength of the shock is high enough to cause a complete reorganisation of the flow behaviour. Thus, the shock strength limit for breakdown for these solutions may be given as 3.73. This appears to confirm the proposal made previously, that the normal shock strength is over-predicted, thus causing the breakdown to occur earlier over the wing for the vortex core behaviour predicted. To determine a link between the vortex flow conditions, as described by the Rossby number, and the shock strength for breakdown to occur on the wing, further data, both experimental and computational, is needed. By considering different flow conditions and configurations a trend similar to Figure 13 may be determined for transonic vortex breakdown.

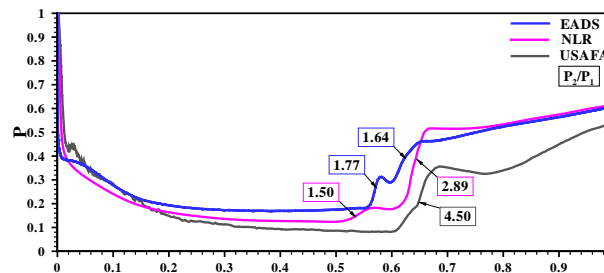


Figure 15. Pressure distribution through vortex cores for EADS, NLR and USAFA solutions

To further consider the relation between the occurrence of breakdown, the vortex core behaviour and the predicted shock strength, the vortex core data for the EADS-MAS, NLR and time averaged USAFA results are considered in a similar manner. The pressure behaviour through the vortex core, with the pressure ratios marked, is shown in Figure 15.

From this plot, it is clear that a similar behaviour occurs, with shocks intersecting the vortex core axis and vortex breakdown occurring. From the EADS-MAS and NLR solutions, the pressure ratios through the shocks are approximately 1.77 and 1.64, and 1.5 and 2.89, respectively. The USAFA time averaged solution has only one shock region with a ratio of 4.5. However, from analysis of the instantaneous solutions, it was found that two shocks also exist at breakdown, which for the solution at a time step of $\tau = 16600$ correspond to 2.25 and 2.71.

While the predicted strength of a shock can be dependent on such factors as grid refinement, turbulence model and solver treatment, it is also apparent that there are corresponding differences in predicted maximum axial velocity through the vortex core, as summarised in Table 4. The current solution has predicted a maximum axial velocity which is the same as the USAFA solutions and higher than for the EADS-MAS and NLR solutions. As a result of this increase in axial velocity the Mach number upstream of the shock will increase, and the upstream pressure will reduce, resulting in a stronger shock to maintain equilibrium of the flow. However, it is evident that the Rossby number in each case is similar. This suggests that the shock strength predicted by the computational solutions is dependent on the vortex core behaviour predicted upstream. The axial flow behaviour is also dependent on the computational parameters mentioned above. However, despite the differences in flow solutions and computational set-up, the behaviour and effect of the shocks on the flow are the same.

	U_{axial}	M_{axial}	Ro	Vortex core Shocks			Shock at	VBD x/c_r
				1st: $\frac{P_2}{P_1}$	2nd: $\frac{P_2}{P_1}$	Total: $\frac{P_2}{P_1}$	$y/s = 0.3$: $\frac{P_2}{P_1}$	
EADS	1.50	-	~ 1.67	1.77	1.64	2.55	1.4274	0.68
Glasgow	1.83	2.00	~ 1.7	2.00	2.36	4.75	1.4695	0.64
NLR	1.60	-	~ 1.74	1.50	2.89	4.33	1.5075	0.67
USAFA (time ave.)	1.80	2.03	~ 1.67	-	-	4.50	1.4409	0.68
USAFA (instant.)	-	-	-	2.51	2.71	4.75	-	0.66

Table 4. Summary of maximum axial velocity, shock strength and breakdown location for all solutions at $\alpha = 23^\circ$, $M = 0.85$ and $Re = 6 \times 10^6$

To consider the ability of the computational solutions to predict the axial flow upstream of breakdown, the PIV results obtained at DLR and described in Konrath *et al.*¹⁴ were considered. These experiments were carried out for a slightly different flow conditions, with a Mach number of $M = 0.80$ and Reynolds number of $Re = 3 \times 10^6$. To compare with these results, a new set of calculations were performed, using the $k - \omega$ with P_ω Enhancer turbulence model for $M = 0.80$ and $Re = 2 \times 10^6$ at angles of incidence of $\alpha = 18.5^\circ - 26^\circ$. Figure 16 shows a comparison of the cross-flow behaviour for a nominal incidence of $\alpha = 26^\circ$. The effect of the difference in Reynolds numbers will be negligible due to the sharp leading edge. In the experiment, it was found that vortex breakdown occurred between the $x/c_r = 0.6$ and 0.7 streamwise stations. However, the computations predict breakdown further upstream at $x/c_r = 0.4$. Therefore, to make a comparison of the pre-breakdown flow, the results were compared on planes which were a similar non-dimensional distance from the breakdown location, this corresponds to $x/c_r = 0.5$ for the experiment and $x/c_r = 0.3$ for the computational results assuming that the breakdown occurs close to the $x/c_r = 0.6$ location. From the comparisons of the non-dimensional u velocity contours, a number of observations may be made. It is clear that the location of the vortex core is very different between the computational and experimental results, however this is likely to be due to the proximity of the computational slice to the apex of the wing as further downstream the vortex would lift further from the wing surface. However, the shape of the vortical system is the same, with a very elongated primary vortex clear for both sets of results. Considering the vortex core properties, from the experimental data at three pre-breakdown PIV planes, it was found that the u velocity corresponds to 1.962 at $x/c_r = 0.5$, 1.870 at $x/c_r = 0.55$ and 1.522 at $x/c_r = 0.6$. Although the maximum velocity found from the measurement planes is 1.962, it is likely that the actual maximum velocity will be larger. This is evident from Figure

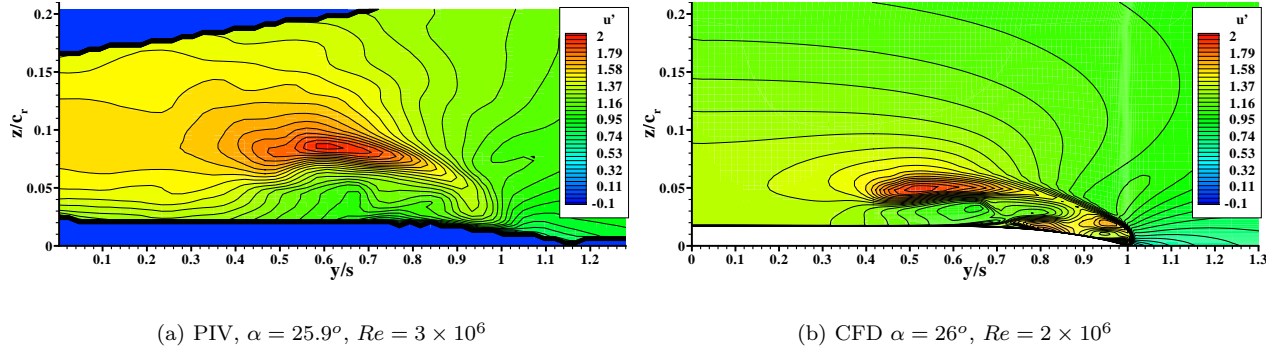


Figure 16. Comparison between u velocity contours for experimental PIV and computational results for $M = 0.80$ on a slice at $x/c_r = 0.5$.

17, which plots these three points along side the velocity behaviour of the computational results. The maximum u velocity for the computational results corresponds to $u = 1.88$, which is slightly lower than the maximum experimental value. Therefore, it is likely that the axial flow behaviour is under-predicted in the computational solutions.

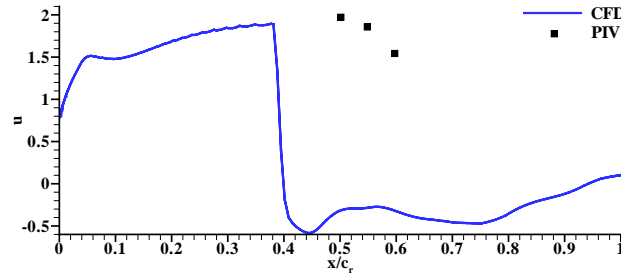


Figure 17. u velocity through vortex core for computational results compared to experimental PIV data for $M = 0.80$, $\alpha = 26^\circ$

Having considered the mechanisms which cause vortex breakdown to occur on the wing, it is possible to return to the issue of the discrepancies between the CFD and experimental results. It was found from the experimental data used in this study that vortex breakdown jumps abruptly from a location downstream of the trailing edge to a location upstream on the wing for a small increases in incidence. Indeed from the results summarised in Table 3, it is clear that the flow seems to go from full vortical flow over the whole wing surface to breakdown occurring close to the $x/c_r = 0.6$ location in a one degree increase.

From the plot in Figure 2 it is clear that the behaviour of the onset of vortex breakdown is very similar for both the CFD and experiment, however the angle at which this occurs varies. With further consideration of the literature it was found that there is a large spread of values for this critical angle. These are detailed in Table 5 below. It is quite clear from all these results that the critical onset angles for vortex breakdown over the wings for current CFD solutions are consistently earlier than for the majority of the experimental results. To explain this difference, further consideration is needed to the discussion given above considering a critical limit for breakdown to occur dependent on the vortex core strength and the strength and locations of the shockwaves in the flow. As shown, with an increase in incidence the strength of the shocks in the flow increases, most likely as a response to the increased acceleration of the flow over the wing surface. Similarly, the axial velocity in the vortex core increases and it has been shown that there is a critical relationship between these quantities which results in breakdown for a critical incidence. To change the angle at which vortex breakdown occurs, it will be necessary to have a change in either one of these parameters. For example, with an increase in vortex intensity and therefore a decrease in axial velocity or an increase in tangential velocity, the strength of the shock needed to

<i>Source</i>	<i>Type</i>	<i>Conditions</i>	α_{cr}
Elsenaar and Hoeijmakers ²	exp.	$M = 0.85, Re = 9 \times 10^6$	23°
Houtmann and Bannink ²¹	exp.	$M = 0.85, Re = 3.6 \times 10^6$	20°
Chu and Luckring ⁹	exp.	$M = 0.799, Re = 6 \times 10^6$	26.6°
"	exp.	$M = 0.831, Re = 6 \times 10^6$	24.6°
"	exp.	$M = 0.851, Re = 6 \times 10^6$	24.6°
"	exp.	$M = 0.871, Re = 6 \times 10^6$	24.7°
"	exp.	$M = 0.9, Re = 6 \times 10^6$	22.6°
"	exp.	$M = 0.849, Re = 11.6 \times 10^6$	24°
Longo ³	CFD	$M = 0.8, \text{Inviscid}$	25°
Glasgow	CFD	$M = 0.85, Re = 6 \times 10^6$	20°
EADS-MAS	CFD	$M = 0.85, Re = 6 \times 10^6$	21°

Table 5. Critical incidence for transonic vortex breakdown to be found on 65° delta wings

cause breakdown will decrease and breakdown will occur earlier on the wing.

From the results detailed in the previous section, it may be suggested that two factors are causing the early prediction of breakdown on the wing. These are an under-prediction of the axial velocity, which results in a vortex more susceptible to breakdown and an over-prediction of the strength of the shocks within the flow. From consideration of the effects of a number of flow parameters, it appears that these predictions are not greatly effected by grid structure, turbulence model, convergence or time accuracy. The effect of grid refinement was also considered, which also concluded that the overall refinement of the grid had little effect on the solution. However, this study did not consider localised refinement, particularly in the vortex core region. Despite continuing improvement in CFD codes, turbulence models and practises, prediction of the vortex core behaviour and axial flow is still a challenge. There have been a number of collaborations and investigations which have considered the vortical flows over delta wings, which have also generally predicted the flow behaviour well, however the axial velocity is almost always much lower than that found from experiments. This is also true for this case and may be attributed to the abilities of turbulence modelling and restrictions in grid refinement for the core region. To fully resolve the vortex core behaviour it would be necessary to have similar refinement as is applied to boundary layer regions. It is unclear at this time whether an improvement in vortex core axial velocity would alter the predicted strength of the shocks in the flow, however, if the shock strength remained constant, with an increase in axial velocity, it may be suggested that the angle of incidence at which breakdown occurred would increase.

V. Conclusions

The following conclusions are drawn

- The sudden motion in breakdown location observed in experiments is due to a shock-vortex interaction.
- The shock which is involved in the interaction is due to the sting, and is hence an example of experimental interference.
- The CFD predictions of the breakdown movement are insensitive to the simulation details.
- The onset angle of the breakdown movement was predicted about 3 degrees earlier than the measurements. The tunnel interference could contribute to this and should be further investigated.
- The reason for this could be due to the prediction of the shock strength or axial flow in the vortex.

- More detailed measurements of surface pressures and flow field velocities are needed to evaluate this point.

VI. Acknowledgements

Lucy Schiavetta acknowledges the sponsorship of BAE SYSTEMS and EPSRC, including grants EP/E009956 and GR/S16485.

References

- ¹Jobe C.E. Vortex breakdown location over 65° delta wings empiricism and experiment. *Aeronautical Journal*, pages 475–482, September 2004.
- ²Elsenaar A and Hoeijmakers H.W.M. An experimental study of the flow over a sharp-edged delta wing at subsonic and transonic speeds. In *AGARD Conference Proceedings “Vortex Flow Aerodynamics”*, pages 15.1–15.19. AGARD-CP-494, July 1991.
- ³Longo J.M.A. Compressible inviscid vortex flow of a sharp edge delta wing. *AIAA Journal*, 33(4):680–687, April 1995.
- ⁴Thomer O, Schröder W, and Krause E. Normal shock vortex interaction. In *Proceedings of the RTO-AVT Symposium on “Advanced Flow Management: Part A - Vortex Flows and High Angle of Attack for Military Vehicles” - RTO-MP-069(I)*, pages 18.1–8.10. NATO RTO, 2001.
- ⁵Donohoe S.R and Bannink W.J. Surface reflective visualisations of shock-wave/vortex interactions above a delta wing. *AIAA Journal*, 35(10):1568–1573, October 1997.
- ⁶Elsenaar A, Hjemberg L, Bütefisch K-A, and Bannink W.J. The international vortex flow experiment. In *Validation of Computational Fluid Dynamics - AGARD-CP-437 Volume 1*, pages 9.1–9.23. AGARD, 1988.
- ⁷Hummel D and Redeker G. A new vortex flow experiment for computer code validation. In *Proceedings of the RTO-AVT Symposium on “Advanced Flow Management: Part A - Vortex Flows and High Angle of Attack for Military Vehicles” - RTO-MP-069(I)*, pages 8.1–8.32. NATO RTO, 2001.
- ⁸Hummel D. Effects of boundary layer formation on the vortical flow above slender delta wings. In *RTO-MP-AVT-111*, pages 30.1–30.22. NATO, October 2004.
- ⁹Chu J and Luckring J.M. Experimental surface pressure data obtained on a 65° delta wing across Reynolds number and Mach number ranges: Volume 1 - sharp leading edge. NASA Technical Memorandum 4645, NASA Langley Research Centre, February 1996.
- ¹⁰Chu J and Luckring J.M. Experimental surface pressure data obtained on a 65° delta wing across Reynolds number and Mach number ranges: Volume 2 - small radius leading edge. NASA Technical Memorandum 4645, NASA Langley Research Centre, February 1996.
- ¹¹Chu J and Luckring J.M. Experimental surface pressure data obtained on a 65° delta wing across Reynolds number and Mach number ranges: Volume 3 - medium radius leading edge. NASA Technical Memorandum 4645, NASA Langley Research Centre, February 1996.
- ¹²Chu J and Luckring J.M. Experimental surface pressure data obtained on a 65° delta wing across Reynolds number and Mach number ranges: Volume 4 - large radius leading edge. NASA Technical Memorandum 4645, NASA Langley Research Centre, February 1996.
- ¹³Boelens O.J. Private communication.
- ¹⁴Konrath R. Private communication.
- ¹⁵Schiavetta L.A, Boelens O.J, and Fritz W. Analysis of transonic flow on a slender delta wing using CFD. In *24th AIAA Applied Aerodynamics Conference*. AIAA Paper 2006-3171, June 2006.
- ¹⁶FLOWer, *Installation and User Handbook*.
- ¹⁷Kok J.C. Mathematical physical model of ENSOLV version 3.20; a flow solver for 3D Euler/Navier-Stokes equations in arbitrary multi-block domains. NLR-CR-2000-620, Nationaal Lucht- en Ruimtevaartlaboratorium, NLR, 2000.
- ¹⁸Kok J.C and Prananta B.B. User guide of ENSOLV version 5.01. a flow solver for 3D Euler/Navier-Stokes equations in arbitrary multi-block domains with aeroelastic capabilities. NLR-CR-2001-348, Nationaal Lucht- en Ruimtevaartlaboratorium, NLR, 2001.
- ¹⁹Badcock K.J, Richards B.E, and Woodgate M.A. Elements of computational fluid dynamics on block structured grids using implicit solvers. *Progress in Aerospace Sciences*, 36:351–392, 2000.
- ²⁰Strang W.Z, Tomaro R.F, and Grismer M.J. The defining methods of cobalt-60: A parallel, implicit, unstructured Euler/Navier-Stokes flow solver. In *37th AIAA Aerospace Sciences Meeting and Exhibit*. AIAA Paper 99-0786, January 1999.
- ²¹Houtman E.M and Bannink B.J. Experimental and numerical investigation of the vortex flow over a delta wing at transonic speeds. In *AGARD Conference Proceedings “Vortex Flow Aerodynamics”*, pages 5.1–5.11. AGARD-CP-494, July 1991.
- ²²Kok J.C. Resolving the dependence on freestream values for the $k - \omega$ turbulence model. *AIAA Journal*, 38(7):1292–1294, 2000.
- ²³Délery J.M. Aspects of vortex breakdown. *Progress in Aerospace Sciences*, 30(1):1–59, 1994.
- ²⁴Kalkhoran I.M and Smart M.K. Aspects of shock wave-induced vortex breakdown. *Progress in Aerospace Sciences*, 36:63–95, 2000.
- ²⁵Spall R.E, Gatski T.B, and Grosch C.E. A criterion for vortex breakdown. *Physics of Fluids*, 30(11):3434–3440, November 1987.
- ²⁶Robinson B.A, Barnett R.M, and Agrawal S. Simple numerical criterion for vortex breakdown. *AIAA Journal*, 32(1):116–122, January 1994.